

RESEARCH

Open Access



# Distinct transcriptomic signatures define febrile malaria depending on initial infective states, asymptomatic or uninfected

Kelvin M. Kimenyi<sup>1,2</sup>, Mercy Y. Akinyi<sup>1</sup>, Kioko Mwikali<sup>1</sup>, Tegan Gilmore<sup>4</sup>, Shaban Mwangi<sup>1</sup>, Elisha Omer<sup>1</sup>, Bonface Gichuki<sup>1</sup>, Juliana Wambua<sup>1</sup>, James Njunge<sup>1</sup>, George Obiero<sup>2</sup>, Philip Bejon<sup>1,3</sup>, Jean Langhorne<sup>4</sup>, Abdirahman Abdi<sup>1</sup> and Lynette Isabella Ochola-Oyier<sup>1\*</sup>

## Abstract

**Background** Cumulative malaria parasite exposure in endemic regions often results in the acquisition of partial immunity and asymptomatic infections. There is limited information on how host-parasite interactions mediate the maintenance of chronic symptomless infections that sustain malaria transmission.

**Methods** Here, we determined the gene expression profiles of the parasite population and the corresponding host peripheral blood mononuclear cells (PBMCs) from 21 children (< 15 years). We compared children who were defined as uninfected, asymptomatic and those with febrile malaria.

**Results** Children with asymptomatic infections had a parasite transcriptional profile characterized by a bias toward trophozoite stage (~ 12 h-post invasion) parasites and low parasite levels, while early ring stage parasites were characteristic of febrile malaria. The host response of asymptomatic children was characterized by downregulated transcription of genes associated with inflammatory responses, compared with children with febrile malaria. Interestingly, the host responses during febrile infections that followed an asymptomatic infection featured stronger inflammatory responses, whereas the febrile host responses from previously uninfected children featured increased humoral immune responses.

**Conclusions** The priming effect of prior asymptomatic infection may explain the blunted acquisition of antibody responses seen to malaria antigens following natural exposure or vaccination in malaria endemic areas.

**Keywords** Malaria, Asymptomatic *Plasmodium falciparum* infection, Immunity, Host-parasite interactions

## Introduction

Malaria remains a global health concern that was responsible for 247 million cases and 619,000 deaths in 2021 [1], despite the availability of a working diagnostic test, effective treatment and the recently licenced vaccine. *Plasmodium falciparum* is the main causative agent of malaria infections in sub-Saharan Africa. During the parasite's life cycle, the merozoite stage that emerges from the liver invades new erythrocytes, developing into rings, trophozoites and finally into multinucleated schizonts containing new merozoites that are released to perpetuate

\*Correspondence:

Lynette Isabella Ochola-Oyier  
lioyier@kemri-wellcome.org

<sup>1</sup> KEMRI-Wellcome Trust Research Programme, Kilifi, Kenya

<sup>2</sup> Department of Biochemistry, University of Nairobi, Nairobi, Kenya

<sup>3</sup> Centre for Tropical Medicine and Global Health, Nuffield Department of Medicine, University of Oxford, Oxford, UK

<sup>4</sup> The Francis Crick Institute, London, UK



© The Author(s) 2024. **Open Access** This article is licensed under a Creative Commons Attribution 4.0 International License, which permits use, sharing, adaptation, distribution and reproduction in any medium or format, as long as you give appropriate credit to the original author(s) and the source, provide a link to the Creative Commons licence, and indicate if changes were made. The images or other third party material in this article are included in the article's Creative Commons licence, unless indicated otherwise in a credit line to the material. If material is not included in the article's Creative Commons licence and your intended use is not permitted by statutory regulation or exceeds the permitted use, you will need to obtain permission directly from the copyright holder. To view a copy of this licence, visit <http://creativecommons.org/licenses/by/4.0/>. The Creative Commons Public Domain Dedication waiver (<http://creativecommons.org/publicdomain/zero/1.0/>) applies to the data made available in this article, unless otherwise stated in a credit line to the data.

the life cycle [2]. The bursting of infected erythrocytes releases merozoites and parasite byproducts that cause fever, a characteristic feature of clinical malaria [3]. In addition, later stages of parasite development (trophozoites and schizonts) in infected erythrocytes introduce parasite proteins, termed variant surface antigens (VSAs), on the erythrocyte cell membrane facilitating cytoadherence. Cytoadherence is the binding, through VSAs, of the infected erythrocyte onto host endothelial cells, which influences parasite virulence and malaria disease severity [4]. Therefore, in the case of asymptomatic infections reduced parasite cytoadherence and increased circulation of parasites in peripheral blood is suggested to be the mechanism maintaining asymptomatic infections, due to the reduction in parasitemia to a level that is tolerable to the immune system [5]. The complex range of host-parasite interactions results in a spectrum of clinical presentations of *P. falciparum* infections from severe, through uncomplicated febrile episodes, to asymptomatic parasite carriers [6, 7].

Due to repeated exposure to malaria, individuals residing in endemic regions acquire partial immunity or are semi-immune to malaria, enabling them to control parasitemia and inflammation [8, 9]. However, this natural partial immunity rarely progresses to sterile immunity and thus individuals are continually infected with the parasite, often resulting in asymptomatic infections [10]. The immunity in asymptomatic individuals has been summarized as antiparasitic immunity that prevents parasite growth and anti-disease immunity that prevents symptoms [11]. However, this advantage of partial immunity is lost in individuals who leave malaria endemic regions [12]. Asymptomatic infections are problematic for malaria control efforts as they often go undetected and act as a reservoir of parasites that perpetuate malaria transmission [6]. They have also been shown to increase the risk of febrile illness in low transmission settings and appear to be protective against febrile disease in high transmission settings [13–15]. Additionally, they may be precursors of symptomatic malaria primarily due to superinfections with new parasite clones [16–19]. Therefore, immune tolerance to the parasite clones circulating during an asymptomatic infection potentially reduces the risk of subsequent febrile infections with the same clone [20]. Furthermore, prior malaria exposure may interfere with vaccine efficacy as malaria exposed adults have been shown to elicit reduced immune responses, particularly antibodies, compared to infants and malaria naïve adults [21, 22].

Asymptomatic malaria infections have previously been explored using transcriptomic studies, which revealed reduced transcription of pro-inflammatory genes [23], inhibition of T-cell function [24] and enhanced p53

pathway expression by monocytes [25]. Other studies have associated these infections with greater levels of immunoregulatory cytokines [26, 27]. Despite the rapid increase in knowledge obtained from clinical malaria isolates, much less is known about gene expression by the parasite and host immune cells during asymptomatic *P. falciparum* infections and the ensuing follow-up febrile infections. In this study, we followed a longitudinal cohort of children with similar history of exposure to infection and sought to understand the biology of asymptomatic infections. We tracked within-host responses and defined, at a single snapshot in time, asymptomatic and uninfected individuals and their ensuing febrile infection pairs. A comparison of the parasite transcriptome and the host PBMCs transcriptome and proteome was conducted between the paired asymptomatic-febrile and uninfected-febrile episodes. The population differences between uninfected, asymptomatic and febrile individuals were also examined. Thus, this study was set out to determine whether detectable asymptomatic infections had an impact on the stages of the parasite in circulation, whether the host immune response differed when compared to that of children from the same cohort with no detectable parasitaemia (uninfected), and whether asymptomatic infection affects the host response to a febrile superinfection.

## Methods

### Study population

This study was conducted in Junju, a moderate to high malaria transmission region in Kilifi County, Kenya. This region experiences two rainy seasons annually, the long rains in April to July and the short rains in October to November, which are characterised by increased malaria transmission [28]. The samples were collected from a cohort of 425 children living in Junju who were recruited at birth and followed up weekly by active surveillance until the age of 15, where *P. falciparum* malaria was diagnosed (using a rapid diagnostic test (RDT) and confirmed with microscopy) and treated [29]. Annual cross-sectional blood surveys were conducted in this cohort before the long rains from 2007 to 2018 and the children were defined as uninfected, asymptomatic, febrile malaria and non-malarial fever.

### Definitions

Uninfected children were defined as being parasite negative by RDT and microscopy. Asymptomatic infections were parasite positive by RDT, and confirmed by microscopy, with an axillary temperature < 37.5 °C and no symptoms of fever, and with no febrile malaria episode within the month up to the survey or the subsequent 7 days after the date of the survey [13,

16]. Sub-microscopic asymptomatic infections were excluded as they yielded insufficient RNA material for RNAseq during optimization assays. For the first-febrile malaria infections from individuals who were initially uninfected their parasitemia was defined as  $\geq 2500$  parasites/ $\mu\text{l}$  by microscopy and a tympanic temperature  $\geq 37.5$  °C based on definitions previously described for this cohort [27] while any parasitaemia by microscopy and a tympanic temperature  $\geq 37.5$  °C was considered for the first-febrile infections from those who were initially asymptomatic. Only microscopy-positive samples were included in this study. A total of 2801 uninfected, 510 asymptomatic and 3205 febrile samples collected between 2009 and 2017 were selected for subsequent analysis. About 154 paired samples from children who were asymptotically infected on the survey and subsequently experienced febrile infections were identified for parasite and PBMC transcriptomic and proteomic analysis but only 21 pairs were available in the biobank. Additionally, 22 paired uninfected and corresponding febrile infections were available for

PBMC transcriptomic and proteomic analysis out of 1500 pairs identified in the database (Fig. 1).

**Sample collection**

Blood samples were drawn by venipuncture from all the participants during the cross-sectional bleed and at their follow-up febrile malaria episode. The samples were collected in sodium citrate-containing cell preparation tubes (Vacutainer CPT Tubes, BD) and transported to the laboratory where they were separated into peripheral blood mononuclear cells (PBMCs) and red blood cell (RBC) pellets, harvested and processed before storage in liquid nitrogen (LN<sub>2</sub>). PBMCs were isolated using the Lymphoprep™ density gradient solution, carefully collected using a wide mouth Pasteur pipette and then washed twice with RPMI media before storage in LN<sub>2</sub>. Each sample was then separated into two components, one for transcriptomics and the other for proteomics.

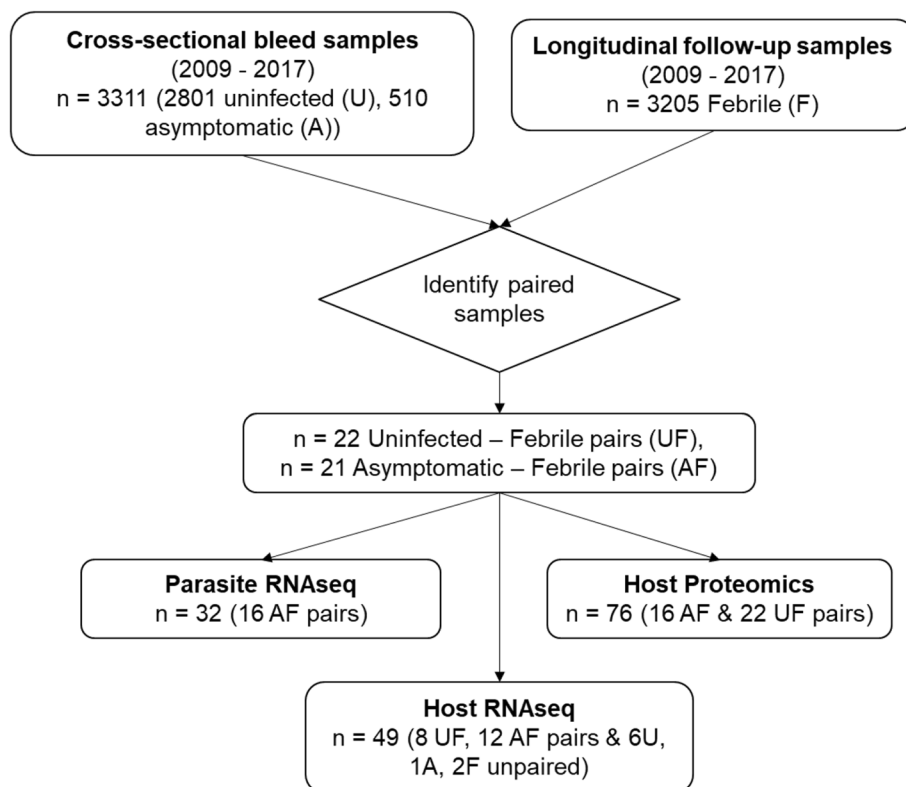


**Fig. 1** A schematic of the sample selection process. Uninfected (U) (*P. falciparum* negative and no malaria symptoms) and asymptomatic (A) (*P. falciparum* positive and no malaria symptoms) samples were collected during the annual cross-sectional bleed surveys between 2007 and 2017. Subsequent febrile malaria episodes (F) (*P. falciparum* parasitemia  $\geq 2500$  parasites/ $\mu\text{l}$  and axillary temperature  $\geq 37.5$  °C) were detected during weekly active surveillance (longitudinal follow-up). *P. falciparum* detection was based on microscopy. Whole blood from all the sample groups were processed and peripheral blood mononuclear cells (PBMCs) isolated. *P. falciparum* infected red blood cells (RBCs) were processed from the A and AF paired samples

### Preparation and sequencing of *P. falciparum* RNA

At the time of the study, infected erythrocytes from the 21 asymptomatic-febrile sample pairs were retrieved and thawed using decreasing concentrations of NaCl (16% (w/v), 1.2% (w/v) and 0.9% (w/v)) to remove the glycerolyte storage medium. The samples were digested using 0.02% (w/v) saponin, and the parasites were separated from RBC components by centrifugation. RNA was extracted using the ISOLATE II RNA Mini Kit (Biolone) and eluted into 40  $\mu$ l RNase-free water. The RNA quality, concentration and purity were assessed using NanoDrop 2000c (Thermo Scientific). mRNA was enriched using the NEBNext™ Poly(A) mRNA magnetic isolation module, and first strand cDNA was synthesized using Superscript III reverse transcriptase (Invitrogen), while the second strand was synthesized using the NEBNext™ RNA Second Strand Synthesis Module (New England Biolabs). Next, 13.5  $\mu$ l of cDNA was prepared into libraries using the NEBNext™ Ultra II FS DNA library preparation kit (New England Biolabs) and amplified in 17 cycles using the KAPA Library Amp Primer mix (KAPA Biosystems) to increase yield. The Agilent DNA 1000 chips on the Agilent TapeStation 2200 system were used to assess the quality and concentration of the libraries, which were then quantified using the KAPA Library Quantification Kit – Complete Kit (ABI Prism) and pooled into equimolar amounts. Paired-end sequencing was performed using the Illumina HiSeq 4000 platform at the Wellcome Sanger Institute (WSI), UK.

Raw sequence reads in fastq file format were assessed for quality and mapped to the reference *P. falciparum* (3D7 strain, PlasmoDB, release 55) genome using Kallisto's v0.46.1 [28] default settings. Only genes with more than 2 counts per million in 10 or more samples were retained. Parasite age hours post-invasion (hpi) was determined using the maximum likelihood estimation method described in [29] with reference data from [30]. Proportions of parasite stages per sample were determined using a mixture model adapted from [31] using reference data from López-Barragán et al., (2011) [32]. Differences between stage proportions of paired samples were analysed using the Wilcoxon rank sum test. Pearson correlation was used to associate the proportion of rings and nonrings with parasitemia. Normalization was performed using the trimmed mean of M values (TMM) normalization in edgeR v3.38.1 [33] and unwanted variation factors were estimated using RUVSeq v1.30.0 [34].

### Transcriptional analysis of host PBMCs

RNA was extracted from host PBMCs from 21 asymptomatic-febrile pairs and 22 uninfected-febrile pairs of host PBMCs and libraries prepared using the same protocol as the parasite samples described above. Paired-end

sequencing was performed on a NovaSeq 6000 (Illumina) system at the Advanced Sequencing Facility at The Francis Crick Institute, UK. The raw fastq files generated were processed using the RNA-Seq pipeline from the NF-core framework (v21.10.6) [35] using STAR (v2.7.10a) [36] aligner and RSEM (v1.3.1) [37] quantification and all other parameters as default. Samples were mapped to the human reference genome version GRCh38 release 95 obtained from Ensembl. Only samples with greater than 10 million aligned reads were considered. Hemoglobin genes described in [38] were removed from the analysis. Genes having 5 counts per million or higher in 13 (number of samples in the least popular group) or more samples were retained and normalized using TMM normalization. To determine differentially expressed genes among the uninfected, asymptomatic and febrile sample groups, gene analysis was performed by fitting a negative binomial generalized log-linear model in edgeR v3.38.1 [33]. The following matrix formula was applied to the edgeR model:  $\sim 0 + \text{treatment} + \text{pair} + \text{batch}$ . Here, 'treatment' aligned to either uninfected, asymptomatic or febrile, 'pair' indicated the pairing of samples per individual; and 'batch' represented the RNA processing batch. Differentially expressed genes were partitioned into four clusters with the least intracluster variation using K-means clustering and plotted using a heatmap. Additional pairwise analyses were conducted to identify differences between two sample groups. Genes in each cluster were used as input during functional overrepresentation analysis to identify enriched pathways using Gene Ontology (GO) and Kyoto Encyclopedia of Genes and Genomes (KEGG) gene sets [39] in clusterProfiler v4.4.4 [40]. Pathways below a Benjamin-Hochberg adjusted *P* value cut of 0.05 were retained. Deconvolution of log-transformed and normalized counts was performed in CIBERSORT v1.04 [41] using the LM22 signature gene set as a reference to determine the proportion of each immune cell per sample [42]. The differences in cellular proportions among the four conditions were then examined.

### Proteomics analysis of PBMCs

Proteins were extracted from PBMCs by resuspending the pellet with 5  $\mu$ l of 6 M UREA (Thermo Scientific). The protein samples were then adjusted with 50 mM triethylammonium bicarbonate (TEAB, Sigma-Aldrich) to 100  $\mu$ l and the protein concentration was determined using the bicinchoninic acid (BCA) protein assay (Thermo Scientific). The protein samples were then reduced with 40 mM dithiothreitol, alkylated with 80 mM iodoacetamide in the dark, and quenched with 80 mM iodoacetamide at room temperature, followed by digestion with 1  $\mu$ g/ $\mu$ l of trypsin [43]. Nine pools, each containing 9

samples and 1 control for batch correction, were prepared by combining 1  $\mu$ l aliquots from each sample. The samples were pooled using a custom randomization R script. The pooled samples were then individually labelled using the Tandem Mass Tag (TMT) 10-plex kit (Thermo Scientific) according to the manufacturer's instructions. One isobaric tag was used solely for the pooled samples and combined with peptide samples labelled with the remaining 9 tags. The labelled peptide pools were then desalted using P10 C18 pipette ZipTips (Millipore) according to the manufacturer's instructions. Eluted peptides were dried in a Speedvac concentrator (Thermo Scientific) and resuspended in 15  $\mu$ l loading solvent (98% H<sub>2</sub>O, 2% acetonitrile, 0.05% formic acid). The peptides were then quantified using a Qubit Protein Assay Kit (Thermo Fisher Scientific) according to the manufacturer's instructions. A standardized protein concentration of 5  $\mu$ g was finally injected into the LC-MS/MS for analysis. The peptides were then loaded onto the liquid chromatograph, separated on reverse-phase analytical column of 75  $\mu$ m x 50 cm C18 (Thermo Scientific) and measured using a Q Exactive Orbitrap mass spectrometer as described by [43]. To identify and quantify proteins, mass spectrometer output files were analyzed using MaxQuant software version 2.0.3.0 [44] by searching against the UniProt human proteome (downloaded on 10/06/2021) using the Andromeda search engine [45]. N-terminal acetylation and methionine oxidations were set as variable modifications while cysteine carbamidomethylation and TMT-10plex labelled N-terminus and lysine were set as fixed modifications. The false discovery rate (FDR) cut-off was set as 0.01 for both proteins and peptides with a minimum length of seven amino acids and was determined by searching a reverse database. Enzyme specificity was set as C-terminal to arginine and lysine with trypsin as the protease. Only up to two missed cleavages were allowed in the database search. Peptide identification was performed with an allowed fragment mass deviation maximum of 20 ppm (parts per million) and an initial precursor mass deviation maximum of 7 ppm. Default parameters for Orbitrap-type data were used. The pooled sample channels were used for batch correction. The 10-plex corrected reported ion intensity matrix was extracted from the protein group output file and used for downstream analysis. Proteins matching the reversed part of a decoy database, potential contaminants and proteins only identified by a modification site were excluded. Differential protein abundance analysis of the labelled sample intensities generated by MaxQuant was performed using PERSEUS v2.05.0 MaxQuant software (MaxPlanck Institute of Biochemistry, Martinsried, Germany) as described in [46]. The differentially expressed proteins were loaded in STRING version 11.5 ([\[string-db.org/\]\(https://string-db.org/\)\) databases for protein-protein interaction and Gene Ontology \(GO\) functional analyses. Statistical significance was set at FDR < 0.05.](https://</a></p></div><div data-bbox=)

## Results

### Malaria case burden in the cohort

Between 2009 and 2017, the cohort's distribution of febrile malaria cases throughout the year showed perennial malaria transmission, with at least 2 peak months per year. The overall trend in malaria cases was consistent, but there was a drastic drop in the prevalence in malaria cases in 2012 (Fig. 2). The proportion of *P. falciparum* positive asymptomatic infections during the cross-sectional bleed from 2009 to 2017 was highest in 2010 at 25.2% and lowest in 2017 at 4.2%.

### Differential parasite expression profiles of asymptomatic infections compared with febrile malaria

Parasite RNA was successfully isolated from 16 asymptomatic (A) and febrile (F), AF paired samples from 12 females and 4 males. The participants had a mean age of 7.5 years (range: 0.8 – 13.4) during the asymptomatic *P. falciparum* infections and were followed for an average of 114.6 days (range: 22–235) before developing malaria symptoms. In contrast, though not significant, individuals who went from uninfected to febrile did so over an average of three months (96 days). The median parasitaemia was significantly lower during asymptomatic infections (1,720 parasites/  $\mu$ l; range: 120 – 220,000) than during febrile infections (19,229 parasites/  $\mu$ l; range: 480 – 1,280,000) ( $P=0.0204$ ) (Additional file 1: Table S1). On average, approximately 15.4 million paired-end reads were generated per sample (range=0.6 – 111 million reads). The median parasite age, as expressed in hours post-infection (hpi) and determined using the maximum likelihood estimation method [29], was statistically higher ( $P=0.0004$ ) in asymptomatic infections (median=11.7 hpi, (inter-quartile range) IQR[10.48–11.9]) compared to febrile infections (median=8.7 hpi, IQR(7.6–9.55)) (Fig. 3A). The estimated proportions of each intraerythrocytic parasite stage were determined using a mixture model [31], revealing a significantly lower ( $P=0.012$ ) proportion of ring stage parasites in asymptomatic infections than in febrile infections (Fig. 3B). Similarly, a statistically significant ( $P=0.0025$ ) bias towards the early trophozoites was revealed in asymptomatic infections (Fig. 3B).

An all-gene expression principal component analysis (PCA) showed a clear distinction between febrile malaria and asymptomatic infections after correcting for library size, parasite blood stage development and unwanted variations (Fig. 4A). The proportion of the rings and non-ring stages versus parasitemia across all samples was

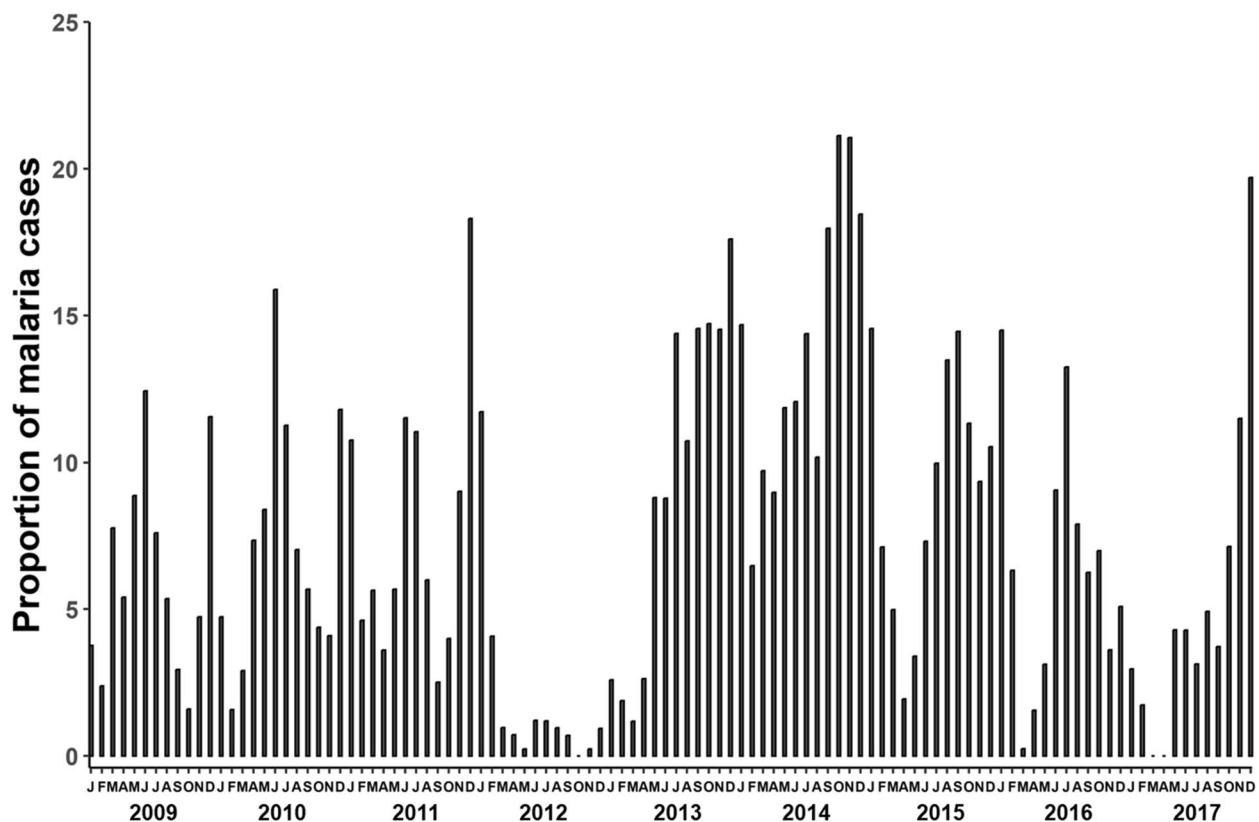


**Fig. 2** Perennial malaria transmission in the Junju cohort. The proportion of symptomatic malaria cases (diagnosed by presence of fever (temperature  $\geq 37.5^{\circ}\text{C}$ ) and parasitemia  $\geq 2500$  parasites/ $\mu\text{l}$ ) recorded in the cohort during the weekly active surveillance. The proportion of malaria cases is the percentage of malaria cases reported per month. The samples were collected from  $\sim 425$  children aged between 0 and 15 years recruited in the Junju cohort

determined whereby the proportion of non-ring parasites was significantly negatively correlated with parasitemia ( $r = -0.45$ ;  $P = 0.01$ ) (Fig. 4B). This indicates that RBCs infected with mature parasite stages circulate longer in low parasitemia.

#### Host PBMC transcriptomes differentiate febrile from non-febrile malaria

A total of 49 PBMC samples from uninfected ( $n = 14$ ), asymptomatic ( $n = 13$ ) and febrile ( $n = 22$ ) individuals were successfully sequenced. Of these, 20 were paired samples, i.e., 8 UF and 12 AF paired samples. The other nine samples were unpaired and comprised 6 uninfected, 1 asymptomatic and 2 febrile samples. The mean age of uninfected individuals (8.15 years) was not significantly different from that of asymptomatic individuals (7.36 years) ( $P = 0.56$ ). There was no significant difference in parasitemia observed between the febrile infections ensuing from uninfected or asymptomatic infections ( $P = 0.504$ ) (Additional file 1: Table S1). On average, approximately 60 million reads mapped to each sample with a range of 11.5 – 374.4 million paired-end reads.

Differential expression analysis revealed 4311 differentially expressed genes (DEGs) (Additional file 1: Table S3). Principal component analysis (PCA) using DEGs separated the samples into febrile and non-febrile groups on PC1, which was associated with 21.64% of the variation, while PC2 (7.52%) partially separated U from A and the febrile infections into those who were initially asymptomatic (FA) and uninfected (FU), suggesting a transcriptional distinction in the febrile infections (Fig. 5A). Gene clustering using DEGs identified four gene clusters 1 to 4 (c1-c4). Overall, c1 (1506 genes) was upregulated in non-febrile children (A and U groups), while c4 (1325 genes) was upregulated in febrile children (FU and FA). There was a marked upregulation of c2 (552 genes) in the FA group and a contrasting pattern of expression in c3, with an upregulation of 928 genes in FU samples (Fig. 5B).

Gene ontology (GO, Fig. 5C-F) and KEGG analysis (Additional file 1: Table S4) produced similar results and were used to determine the predominant functions enriched in each cluster. GO terms for cytoplasmic translation, ribosomal activity, T cell activation and cell adhesion (Fig. 5C) predominated in c1, including genes

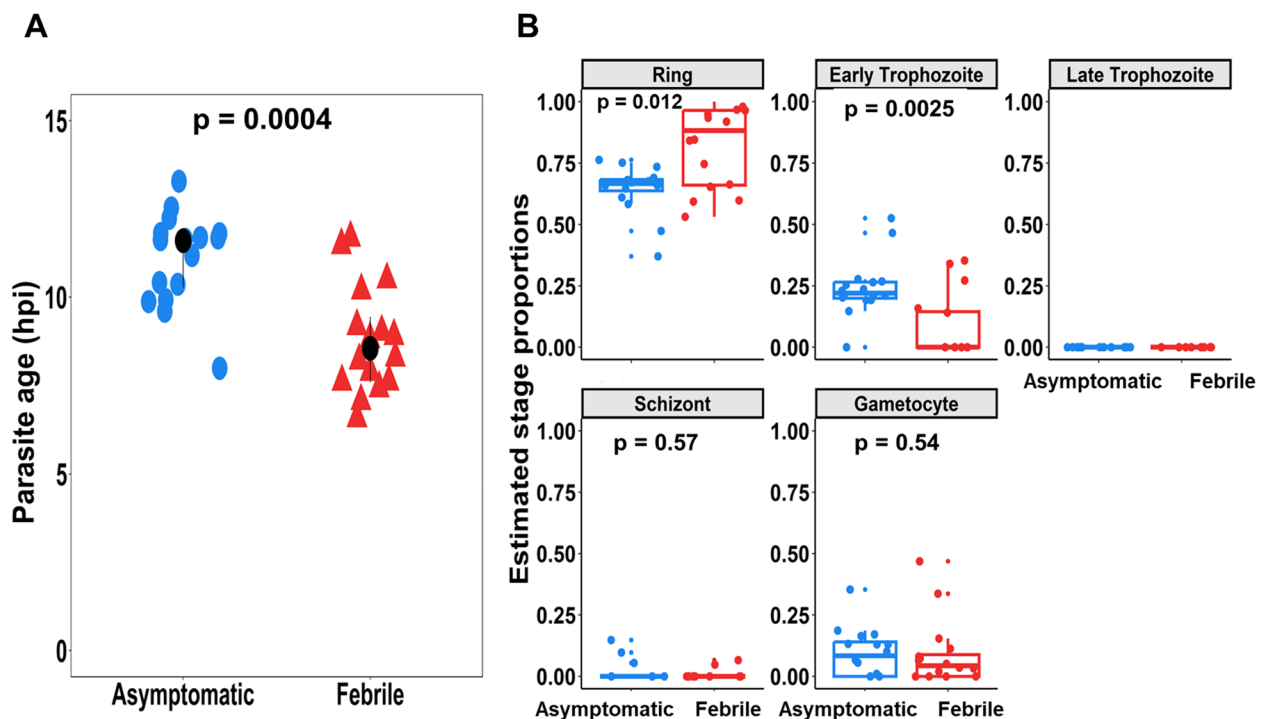


**Fig. 3** Asymptomatic infections are characterized by older, non-ring parasites compared to ensuing febrile malaria. **A** Dot plot showing the maximum likelihood estimation (MLE) of the hours post-invasion (hpi) determined using reference dataset from Bozdech et al. 2003. The samples are colored by clinical phenotype, asymptomatic infections (blue) and febrile malaria (red). The black dot shows the median hpi. **B** Boxplots showing the estimated proportions of parasite blood stage development in asymptomatic infections and febrile malaria as estimated using a mixture model and reference dataset from López-Barragán et al. (2011). For each parasite stage, Wilcoxon test (corrected for multiple testing using Benjamini & Hochberg) was performed to evaluate the difference in the proportions of parasites between asymptomatic and febrile malaria. The samples are colored by clinical phenotype, blue for asymptomatic infections and red for febrile malaria

associated with protein translation factors (EIF3D, EIF3E, EIF3G and EIF3K) and ribosomal proteins (RPL18A, RPL19, RPS12, RPS16, RPL35, RPL8, RPS11, RPS27A) and genes associated with T cell activation and adhesion (CD3D, CD3E, CD3G, CD4, CD96, CD247, CD5, ZAP70, LCK, CXCR4, CXCR5, CD74 and TBX21, GATA3), Figs. 6B and C. These data suggest that protein synthesis and T cell activation were downregulated in the febrile cases.

In contrast, c4 genes were enriched for GO terms involving immune effector processes, adaptive and innate immunity and cytokine pathways (TLR2, STAT3, IL6, IL6R, ANXA3, S100A11, CXCR1, C3AR1, LRG1, S100A8, S100A12, S100A9, JAK3) and regulation of immunity (CD274, CD276, IL1RN, IL10, CR1, CD55, IDO1, IL2RA, BST2) (Fig. 5F). These data show, as expected, that markers of immune activation, particularly neutrophil are upregulated in febrile infections (FA and FU).

The deconvolution analysis revealed some significant differences in the estimated proportions of nine cell types in PBMCs among the four clinical groups. A

lower proportion of naïve B cells was observed in FA, while a higher proportion of plasma cells was observed in the FU group. The proportion of CD8<sup>+</sup> T cells was greatest in U and A; on the other hand, that of naïve and activated memory CD4<sup>+</sup> T cells was greatest in FA and FU. A higher proportion of activated mast cells was also observed in the FA group (Fig. 6).

#### Distinctions in febrile and non-febrile infections

Clusters 2 and 3 drive the separation of febrile infections based on whether they were initially from asymptomatic or uninfected individuals. Cluster 2 was enriched for GO terms involving immune effector processes, leucocyte migration, host defense and TNF production (Fig. 5D). The greatest differences in expression were in the FA group, particularly in genes associated with innate immune effector processes (TLR4, CD14, CD68, TGFB1, EOMES, CCR7, CCL3R1, CD84, TNFRSF1B, IL1B, IFNGR1). There were also some differences between the A and U groups, and a pairwise analysis of the two groups revealed an upregulation of several genes related to inflammatory responses

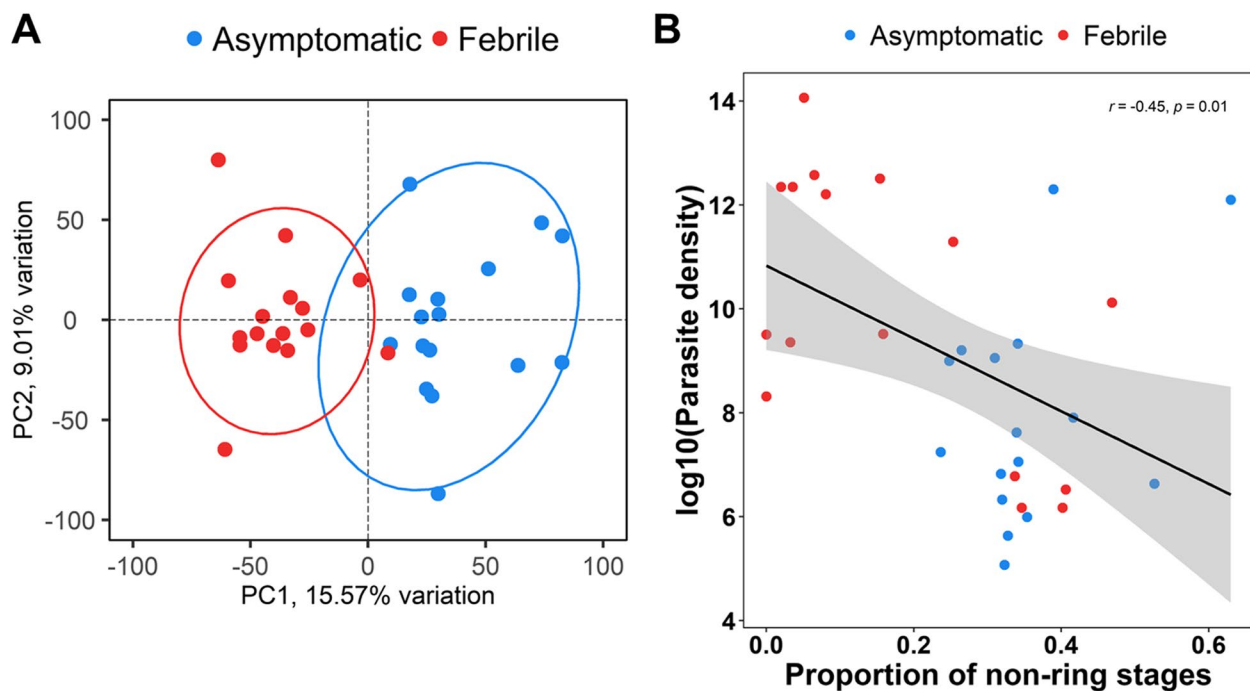


**Fig. 4** Genome-wide expression deconvolution of parasite RNAseq data. **A** Principal component analysis (PCA) of parasite RNA-seq data from paired asymptomatic and febrile malaria normalized for library size, parasite blood stage development and 3 factors of unwanted variation (normalized counts available in (Additional file 1: Table S2)). The samples are colored by the clinical phenotype, blue for asymptomatic infections and red for febrile malaria. Ellipses represent 95% confidence intervals. **B** Scatter plot showing the correlation between the parasite density ( $\log_{10}$ ) and the estimated proportions of non-ring stages across all the samples. The samples are colored by the clinical phenotype, blue for asymptomatic infections and red for febrile malaria

(CCR7, CCL2, NOD2, SIRPA, TNFSF14, NFKB1) in the U group (S5 Table). The innate and inflammatory responses were strongly upregulated in FA compared to the FU group.

The GO terms enriched in c3 were nuclear division and chromosomal segregation, humoral responses, genes for pathways associated with cell cycle regulation (E2F5, CCNA2, CDC6, CDC14B, CCNB1, CDKN2C), and immunoglobulin, phagocytosis and complement (IGHM, IKC, IGHG4, IGHG2, C5) (Fig. 5E). There was a clear distinction in the gene expression of c3 genes between the FA and FU samples, where many genes were upregulated in the FU samples (Fig. 5B), indicating a relatively stronger humoral response. Pairwise analysis of the A and U groups revealed an upregulation

of humoral responses (C1QB, IGHG4, IGKC, IGLC3, IGHV5-51, IGHV3-15, IGHV3-21) in the A group ((Additional file 1: Table S5).

A summary of the 10 most highly differentially expressed genes for the gene ontology terms, humoral responses, cytokines, TNF and T-cell activation in each group is shown in Fig. 7A, with a comparison of the normalized expression of a selection of relevant genes (Fig. 7B). Both the A and U samples show upregulated T-cell activation compared to the respective febrile samples. The FU samples had the strongest expression of immunoglobulin-related genes and humoral response whereas the FA samples had the greatest gene expression for cytokines and TNF production.

(See figure on next page.)

**Fig. 5** Host PBMC gene expression and functional analysis. **A** Principal-component analysis of the 4,311 differentially expressed genes (DEGs) among the four clinical phenotypes. Ellipses represent 95% confidence intervals. Percentages along x and y axes show the degree of variance explained by each principal component. The samples are coloured by the clinical phenotype i.e. A = Asymptomatic, U = Uninfected, FU = Febrile malaria ensuing from uninfected individuals and FA = febrile malaria ensuing from asymptomatic individuals. **B** Heatmap of the 4,311 DEGs (rows) among the four clinical phenotypes (columns) split into 4 clusters using K-means clustering and labelled c1 – c4. **C, D, E** and **F** Barplots showing enriched Gene Ontology (GO) terms in clusters c1, c2, c3 and c4, respectively, from the heatmap in **B**



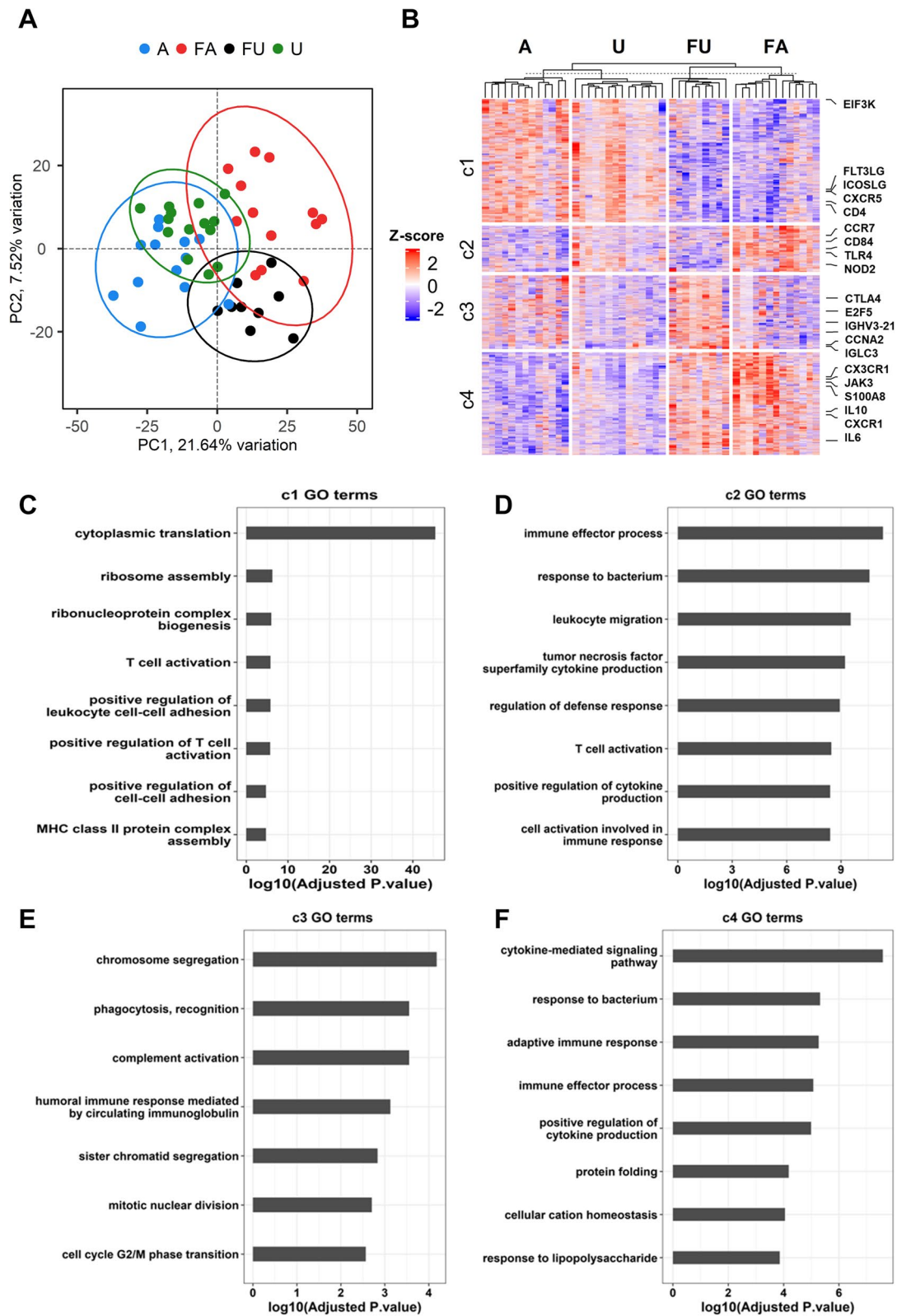


**Fig. 5** (See legend on previous page.)

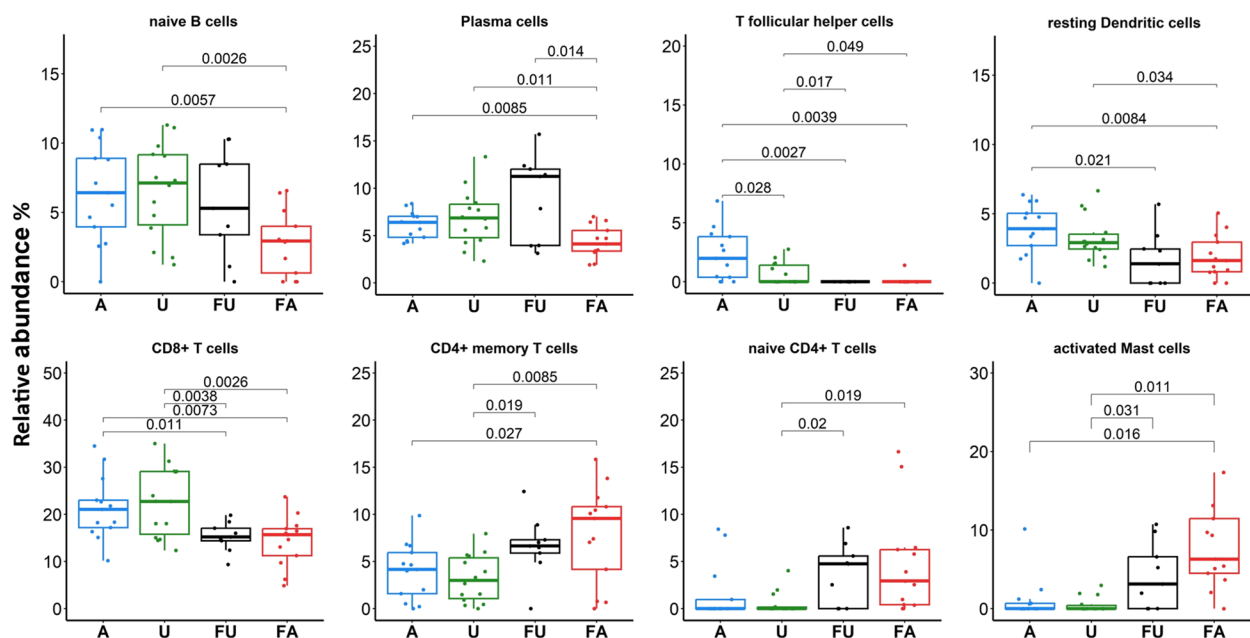


**Fig. 6** Deconvolution of PBMC cell types. PBMC subpopulation proportions were estimated for each sample using the deconvolution analysis in CIBERSORT and a gene signature matrix. Samples are coloured based on the clinical phenotype: A = Asymptomatic, U = Uninfected, FU = Febrile malaria ensuing from uninfected individuals and FA = febrile malaria ensuing from asymptomatic individuals. All pairwise statistical tests indicated in the plots are Wilcoxon tests corrected for multiple testing (Benjamini & Hochberg)

**PBMC proteome distinguishes uninfected, asymptomatic and febrile states**

A paired analysis of PBMC samples from 16 FU pairs and 22 FA pairs was performed using TMT proteomics technology to examine differentially expressed proteins. A total of 318 proteins were identified (q-value < 0.1) after filtering out contaminant proteins. Differential protein expression analyses identified 35 proteins (Fig. 8A and Additional file 1: Table S6). Protein–protein interactions (PPI) analysis in the STRING database revealed significant enrichment of proteins in either the febrile or non-febrile groups (PPI enrichment *P* value < 0.001) (Fig. 8B). Consequently, 16 proteins were upregulated in the non-febrile samples and were enriched for protein-DNA complex and nucleosome (HIST1H1E, HIST1H2BC, H2AFJ, HIST1H4A) cellular components (Fig. 8C). The remainder were upregulated in febrile infections and were enriched for chemokine production (MPO, HP, S100A8, MMP9, ANXA1, DEFA1), neutrophil aggregation and

chemotaxis (S100A8, S100A9, S100A12) and chronic inflammatory response (CAMP, S100A8) biological processes (Fig. 8C). Although a low number of proteins were detected, it indicates chromatin changes in asymptomatic and uninfected individuals, and innate immune responses in febrile infections.

**Discussion**

The longitudinal cohort provided a unique opportunity to follow up individuals with asymptomatic *P. falciparum* infections until they developed symptomatic malaria. The parasite transcriptomic profile in these individuals highlighted an association between non-ring stages and lower parasitemia levels. This is consistent with the abundance of trophozoite stages (average of 12 hpi) in asymptomatic infections. In contrast, febrile infections showed a bias towards ring stage parasites. These observations have been made before in a similar study in Mali [5], reinforcing the idea that parasites adapt to their host, irrespective

(See figure on next page.)

**Fig. 7** Analysis of selected Gene Ontology (GO) terms. **A** Heatmap showing the top 10 differentially expressed genes (DEGs) (based on FDR) enriched in humoral responses, cytokine signaling, TNF production and T cell activation GO terms. The genes (rows) are grouped by the clinical phenotype: A = Asymptomatic, U = Uninfected, FU = Febrile malaria ensuing from Uninfected, FA = Febrile malaria ensuing from Asymptomatic. **B** Boxplots showing the normalized expression levels of selected DEGs per GO term. The boxplots are labelled based on the clinical phenotype: A = Asymptomatic, U = Uninfected, FU = Febrile malaria ensuing from U and FA = febrile malaria ensuing from A. Pairwise statistical analyses indicated in the plots are Wilcoxon tests corrected for multiple testing (Benjamini & Hochberg, \* = < 0.05, \*\* = < 0.01 and \*\*\* = < 0.001)

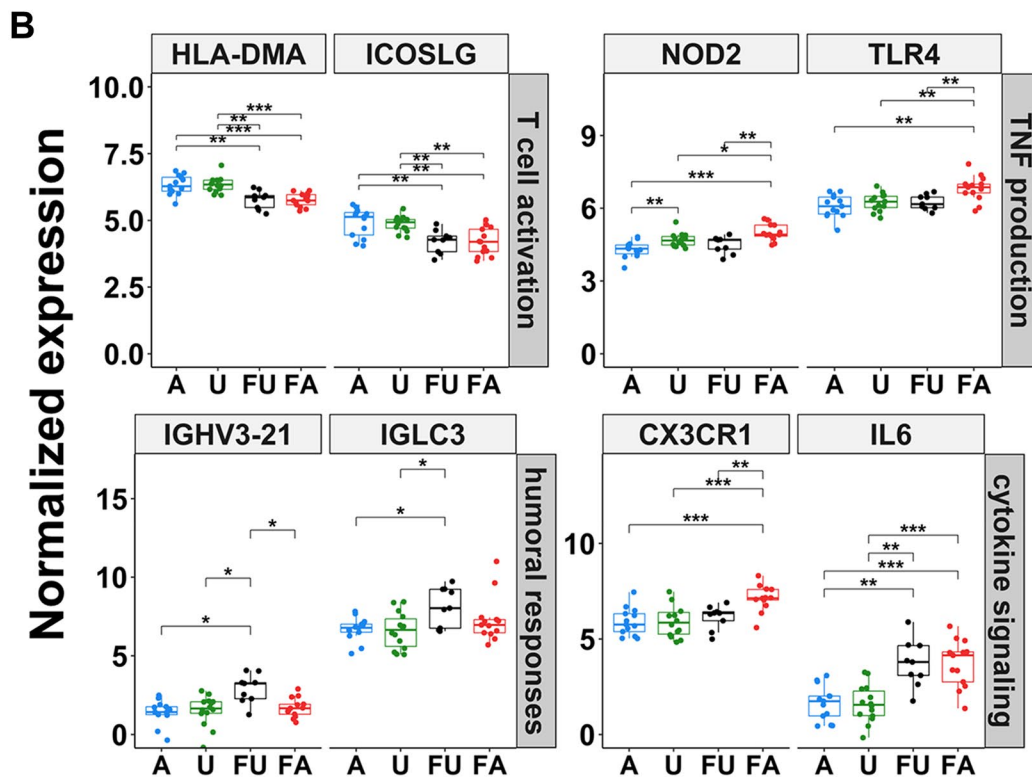
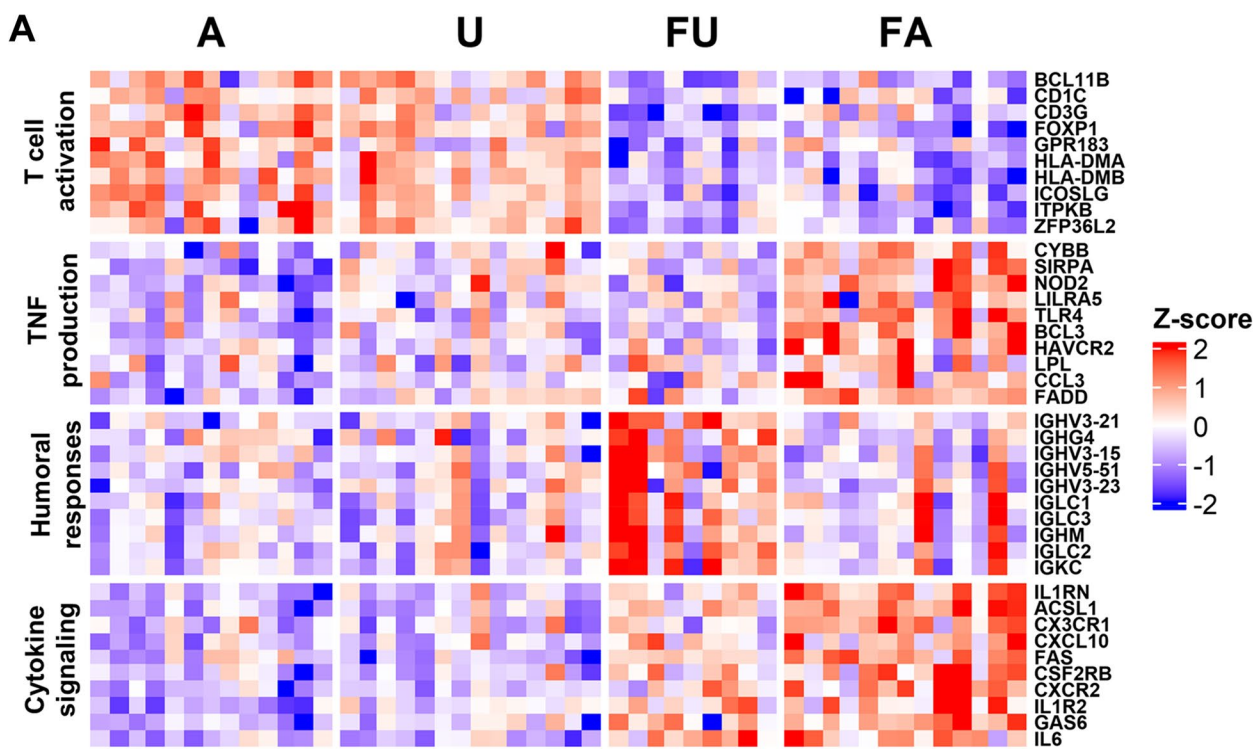
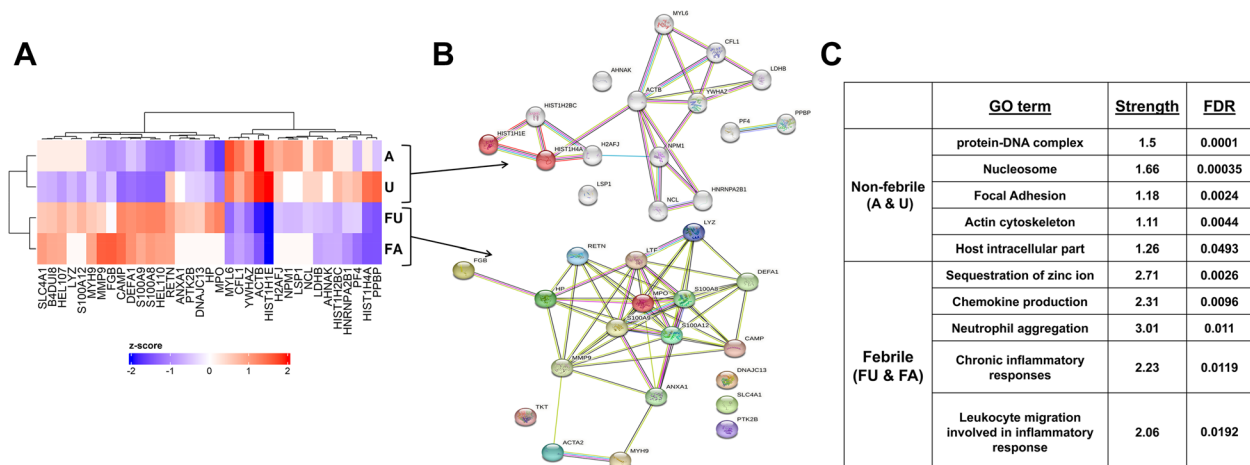


Fig. 7 (See legend on previous page.)



**Fig. 8** Differential expression of proteins among FA and FU pairs. **A** Heat map of the 35 significantly differentially expressed protein in the clinical phenotypes identified using isobaric labeling-based on quantitative proteomics. The columns represent the proteins and the rows the clinical phenotypes, A (Asymptomatic), U (Uninfected) and F (Febrile from Asymptomatic [FA] and Uninfected [FU]). **B** Protein–protein interaction network analysis using STRING database. Proteins are shown as nodes, and the color of each link is based on the type of evidence available for the interaction between two proteins (e.g., purple- experimental, light blue – homology, blue – cooccurrence, black – coexpression, purple – experimental, green – text mining). **C** Gene ontology analysis in STRING database. Strength is a measure of the enrichment effect while FDR is the adjusted *P*-value after correcting for multiple testing using the Benjamini-Hochberg

of differences in malaria transmission. Malaria transmission in Mali is defined by a sharply distinct dry season with very little malaria transmission that switches in the rainy season to a massive upsurge in malaria infections [47]. Along, the Kenyan Coast, the study region, malaria transmission is essentially perennial, demonstrating that the malaria parasite adapts by modifying its host to ensure sustained malaria transmission and parasite survival. This is further demonstrated by a similar profile of increased ring stage parasites previously observed in severe and cerebral malaria cases compared to those from non-severe malaria [31, 48]. The latter infections were skewed towards the early trophozoite stages [31]. The survival of the parasite that is linked to the different portrayal of erythrocyte parasite stages and the disease spectrum (asymptomatic, mild and severe) has previously been attributed to parasite virulence and the ability of the parasite to cytoadhere to host epithelial cells, which potentially dictates the severity of malaria infection outcomes [49]. Increased cytoadherence may result in higher parasitemia and increased malaria severity [5]. This brings to the fore the potential role of VSAs; antibodies against these proteins have been shown to select against parasites with high binding ability [50, 51], hence inadvertently selecting for parasites with low binding ability in semi-immune asymptomatic carriers. These parasites with lower binding ability will predominate and circulate for a longer time in the bloodstream, increasing the splenic clearance of infected erythrocytes [5] and reducing parasitemia. The potential role of VSAs in

maintaining asymptomatic infections should be examined further, since it was not within the scope of this study. An important contributing factor to the differences between asymptomatic and febrile infections could be how the parasite adapts to the host environment which is still not well understood [52–54].

The febrile infections featured a significant increase in parasitemia, which coincides with a preponderance of ring stage parasites, agreeing with similar studies in Mali [5] and Cameroon [55]. The high levels of parasitemia and superinfection with new clones (recently demonstrated in this cohort using *msp2* genotyping and amplicon sequencing of *ama1* [15, 16]) is likely to expose the host to parasite components unfamiliar to the immune system, stimulating more of a ‘primary’ inflammatory-type response, facilitating some control of the high parasitemia clearance, but which may contribute to symptomatic/febrile malaria [56]. The analysis of gene expression profiles from PBMCs in this study, showed that febrile infections were indeed characterized by the upregulation of immune pathways related to immune effector functions, production of inflammatory cytokines, and humoral responses. These results agree with previous studies that compared pre-infection and early febrile malaria infection and revealed a marked activation of pro-inflammatory response pathways in febrile infections [22, 23, 57].

The transcriptomic analyses of febrile infections were surprisingly segregated based on whether the febrile malaria infection was preceded by an asymptomatic

infection or from those who were uninfected. Febrile infections ensuing from asymptomatic infections were characterized by a greater enrichment of genes involved in innate immune processes. In contrast, febrile infections in previously uninfected individuals were characterized by a greater upregulation of humoral immune responses. The increase in transcripts associated with humoral immunity could be due to the higher proportions of plasma cells seen in the deconvolution analysis rather than increased transcription on a per-cell basis; single-cell gene transcriptional analysis would clarify this. Strong inflammatory responses have previously been shown to impair the ability of T follicular helper cells to activate B cells to produce antibodies in the germinal centers [58–60]. Altogether, it is not clear why febrile infections in previously uninfected individuals showed a greater upregulation of gene expression characteristic of B cells and humoral responses. However, plasma antibody responses were not measured, which might reflect more accurately the humoral response. It could be, as suggested by the RNA data, that IgM producing B-cells characteristic of a more primary response, are elevated in the uninfected group, suggesting a less well-developed state of acquired immunity. A longitudinal study incorporating parasite levels, cellular studies and antibody responses would go some way to addressing this.

Prior to febrile infections, the gene expression profiles of asymptomatically infected children and uninfected children were broadly similar. However, the asymptomatic samples did show greater expression of some genes associated with the humoral response compared to uninfected children, perhaps indicating that persistent infection may stimulate greater antibody responses [61]. It is also possible that the immune response has been modified to tolerate the continued parasite presence, and therefore, this would be important to investigate in detail. Our data are similar to previous observations showing gene pathways involved in the production of pro-inflammatory cytokines that were least activated in asymptomatic individuals compared to uninfected individuals [22] and febrile malaria [21].

## Conclusions

Asymptomatic carriers are associated with downregulation of inflammatory responses. In contrast, their ensuing febrile infection appeared to elicit increased inflammatory responses compared to febrile infections ensuing from uninfected individuals. The clear segregation of febrile outcomes based on whether the preceding state was uninfected or asymptomatic provides further evidence that the presence of parasitemia in asymptomatic individuals modifies the host, offering an immunological advantage to the children. However, impaired

antibody responses among asymptomatic individuals upon superinfection align with the reduced malaria vaccine efficacy observed among malaria exposed individuals in endemic regions. Therefore, to achieve malaria elimination, malaria control campaigns should aim to eliminate all parasites, including those in asymptomatic individuals.

## Abbreviations

PBMCs	Peripheral blood mononuclear cells
VSAs	Variant surface antigens (VSAs)
Hpi	Hours post-infection
DEGs	Differentially expressed genes
IQR	Interquartile range
TMM	Trimmed mean of M values
PCA	Principal component analysis
PPI	Protein–protein interactions
GO	Gene Ontology
KEGG	Kyoto Encyclopedia of Genes and Genomes

## Supplementary Information

The online version contains supplementary material available at <https://doi.org/10.1186/s12879-024-08973-2>.

**Additional file 1: S1 Table.** Participants metadata. **S2 Table.** Normalized parasite RNAseq read counts of 16 AF pairs. **S3 Table.** Differentially expressed host PBMC genes across A, U and F groups. **S4 Table.** Functional GO and KEGG analysis of host PBMC genes. a) KEGG analysis results from genes differentially expressed in each cluster. b) Gene Ontology (GO) analysis results from genes differentially expressed in each cluster. P<sub>adj</sub> represents the Benjamini-Hochberg adjusted P-values and was used to sort the GO terms. BP represents the Biological Process category. **S5 Table.** Differentially expression analysis of host PBMC genes between A and U groups. **S6 Table.** Differentially expressed analysis of host PBMC proteins across paired AF and UF groups.

## Acknowledgements

The authors are grateful to the study participants and sincerely appreciate their parents/guardians. We would like to thank the Advanced Sequencing Facility at the Francis Crick Institute for their help with sequencing of the PBMC samples. This manuscript was written with the permission of Director KEMRI CGMRC.

## Authors' contributions

KMK: Conception and design, acquisition of data, analysis and interpretation of data, drafting and revising the manuscript. MA: acquisition and interpretation of data and revising the manuscript. KM: acquisition of data, analysis and interpretation of data and revising the article. TG: analysis and interpretation of data and revising the article. SM, EO, BG and JW: acquisition of data, revising the manuscript. JN: acquisition of data, interpretation of data and revising the manuscript. GO, PB and JL: conceptualization and design, interpretation of data and revised the manuscript. AA and LIO-O: conceptualization and design, interpretation of data, drafting and revising the manuscript. All authors read and approved the final manuscript.

## Funding

This work was supported through the DELTAS Africa Initiative (Grant No. DEL-15-003), an independent funding scheme of the African Academy of Sciences (AAS) Alliance for Accelerating Excellence in Science in Africa (AESA) and supported by the New Partnership for Africa's Development Planning and Coordinating Agency (NEPAD Agency) with funding from the Wellcome Trust and the UK government, DELGEME Grant 107740/Z/15/Z to support KK. The views expressed in this publication are those of the author(s) and not necessarily those of AAS, NEPAD Agency, Wellcome Trust or the UK government. Jean Langhorne is supported by the Francis Crick Institute which receives its

core funding from Cancer Research UK (CC2079), the UK Medical Research Council (CC2079), and the Wellcome Trust (CC2079). There was also support from Wellcome Trust Intermediate Fellowships, Grant Numbers 107568/Z/15/Z and 209289/Z/17/Z awarded to LIO-O and AA, respectively.

#### Availability of data and materials

Parasite and host RNAseq data and processed counts have been deposited in the National Center of Biotechnology Information's Gene Expression Omnibus (GEO) available under GEO accession number GSE240643 and GSE241467, respectively. All mass spectrometry raw files associated with this study are provided in the online Dryad repository ([https://datadryad.org/stash/share/8jLf\\_ceeQfJ8B1FTcGLyZXYu-RQ4c7yddZw2PA4BugE](https://datadryad.org/stash/share/8jLf_ceeQfJ8B1FTcGLyZXYu-RQ4c7yddZw2PA4BugE)).

#### Declarations

##### Ethics approval and consent to participate

Written informed consent was obtained from parents/guardians of the study participants prior to their inclusion in the study. Ethical approval was sourced from the Kenya Medical Research Institute (KEMRI) Scientific Ethics and Review Unit (SERU), under protocol number 3149.

##### Competing interests

The authors declare no competing interests.

Received: 21 September 2023 Accepted: 1 January 2024

Published online: 29 January 2024

#### References

- WHO. World malaria report 2022. 2022.
- Aravind L, Iyer LM, Wellem TE, Miller LH. Plasmodium biology: genomic gleanings. *Cell*. 2003;115(7):771–85.
- Oakley MS, Gerald N, McCutchan TF, Aravind L, Kumar S. Clinical and molecular aspects of malaria fever. *Trends Parasitol*. 2011;27(10):442–9.
- Miller LH, Ackerman HC, Su XZ, Wellem TE. Malaria biology and disease pathogenesis: insights for new treatments. 2013;19(2):156–67.
- Andrade CM, Fleckenstein H, Thomson-luque R, Doumbo S, Lima NF, Anderson C, et al. Increased circulation time of Plasmodium Falciparum underlies persistent asymptomatic infection in the dry season. *Nat Med*. 2020;26:1929–40.
- Galatas B, Bassat Q, Mayor A. Malaria parasites in the Asymptomatic: looking for the Hay in the Haystack. *Trends Parasitol*. 2016;32(4):296–308.
- Doolan DL, Dobaño C, Baird JK. Acquired immunity to malaria. *Clin Microbiol Rev*. 2009;22(1):13–36 (Table of Contents).
- Medzhitov R, Schneider DS, Soares MP. Disease tolerance as a defense strategy. *Science*. 2012;335(6071):936–41.
- Mendonca V, Barral-Netto M. Immunoregulation in human malaria: the challenge of understanding asymptomatic infection. *Mem Inst Oswaldo Cruz*. 2015;110(8):945–55.
- Tran TM, Li S, Doumbo S, Doumbo D, Huang CY, Dia S, et al. An intensive longitudinal cohort study of Malian children and adults reveals no evidence of Acquired immunity to Plasmodium falciparum infection. *Clin Infect Dis*. 2013;57(1):40–7.
- Langhorne J, Ndungu FM, Sponaas AM, Marsh K. Immunity to malaria: more questions than answers. *Nat Immunol*. 2008;9(7):725–32.
- Bediako Y, Adams R, Reid AJ, Valletta JJ, Ndungu FM, Sodenkamp J, et al. Repeated clinical malaria episodes are associated with modification of the immune system in children. *BMC Med*. 2019;17(1):1–14.
- Wamae K, Wambua J, Nyangweso G, Mwambingu G, Osier F, Ndung'u F, et al. Transmission and age impact the risk of developing Febrile Malaria in Children with asymptomatic Plasmodium Falciparum Parasitemia. *J Infect Dis*. 2018;219:936–44.
- Buchwald AG, Sixpence A, Chimanya M, Damson M, Sorkin JD, Wilson ML, et al. Clinical implications of asymptomatic plasmodium falciparum infections in Malawi. *Clin Infect Dis*. 2019;68(1):106–12.
- Wamae K, Kimenyi KM, Osoti V, de Laurent ZR, Ndwiwa L, Kharabora O, et al. Amplicon sequencing as a potential surveillance tool for complexity of infection and drug resistance markers in Plasmodium Falciparum Asymptomatic infections. *J Infect Dis*. 2022;226(5):920–7.
- Kimenyi KM, Wamae K, Ngoi JM, de Laurent ZR, Ndwiwa L, Osoti V, et al. Maintenance of high temporal Plasmodium falciparum genetic diversity and complexity of infection in asymptomatic and symptomatic infections in Kilifi, Kenya from 2007 to 2018. *Malaria Journal*. 2022;21(1):1–10.
- Kun JFJ, Missinou MA, Lell B, Sovric M, Knoop H, Bojowald B, et al. New emerging Plasmodium falciparum genotypes in children during the transition phase from asymptomatic parasitemia to malaria. *Am J Trop Med Hyg*. 2002;66(6):653–8.
- Rono J, Osier FHA, Olsson D, Montgomery S, Mhoja L, Rooth I, et al. Breadth of anti-merozoite antibody responses is Associated with the genetic diversity of asymptomatic Plasmodium Falciparum infections and Protection Against Clinical Malaria. *Clin Infect Dis*. 2013;57(10):1409–16.
- Sissoko MS, Healy SA, Katile A, Omaswa F, Zaidi I, Gabriel EE, et al. Safety and efficacy of PfSPZ Vaccine against Plasmodium Falciparum via direct venous inoculation in healthy malaria-exposed adults in Mali: a randomised, double-blind phase 1 trial. *Lancet Infect Dis*. 2017;17(5):498–509.
- Jongo SA, Church LWP, Mtoro AT, Chakravarty S, Ruben AJ, Swanson PA, et al. Safety and differential antibody and T-cell responses to the plasmodium falciparum sporozoite malaria vaccine, PfSPZ vaccine, by age in Tanzanian adults, adolescents, children, and infants. *Am J Trop Med Hyg*. 2019;100(6):1433–44.
- Tran TM, Jones MB, Ongoiba A, Bijker EM, Schats R, Venepally P, et al. Transcriptomic evidence for modulation of host inflammatory responses during febrile Plasmodium Falciparum malaria. *Sci Rep*. 2016;6: 31291.
- Studniberg SI, Ioannidis LJ, Utami RAS, Trianty L, Liao Y, Abeysekera W, et al. Molecular profiling reveals features of clinical immunity and immunosuppression in asymptomatic P. falciparum malaria. *Mol Syst Biol*. 2022;18(4): e10824.
- Tran TM, Guha R, Skinner J, Ongoiba A, Bhardwaj J, Jones M, et al. Resource a molecular signature in blood reveals a role for p53 in regulating Malaria-Induced inflammation resource a molecular signature in blood reveals a role for p53 in regulating Malaria-Induced inflammation. *Immunity*. 2019;51(4):750–765.e10.
- Jagannathan P, Eccles-James I, Bowen K, Nankya F, Auma A, Wamala S, et al. IFN $\gamma$ /IL-10 Co-producing Cells Dominate the CD4 Response to Malaria in Highly Exposed Children. *PLoS Pathog*. 2014;10(1):e1003864 (Langhorne J, editor).
- Jagannathan P, Kim CC, Greenhouse B, Nankya F, Bowen K, Eccles-James I, et al. Loss and dysfunction of V $\delta$ 2 $^{+}$   $\gamma\delta$  T cells are associated with clinical tolerance to malaria. *Sci Transl Med*. 2014;6(251):251ra117.
- O'Meara WP, Bejon P, Mwangi TW, Okiro EA, Peshu N, Snow RW, et al. Effect of a fall in malaria transmission on morbidity and mortality in Kilifi, Kenya. *Lancet*. 2008;372(9649):1555.
- Mwangi TW, Ross A, Snow RW, Marsh K. Case definitions of clinical malaria under different transmission conditions in Kilifi District, Kenya. *J Infect Dis*. 2005;191(11):1932–9.
- Bray NL, Pimentel H, Melsted P, Pachter L. Near-optimal probabilistic RNA-seq quantification. *Nat Biotechnol*. 2016;34(5):525–7.
- Lemieux JE, Gomez-Escobar N, Feller A, Carret C, Amambua-Ngwa A, Pinches R, et al. Statistical estimation of cell-cycle progression and lineage commitment in Plasmodium Falciparum reveals a homogeneous pattern of transcription in ex vivo culture. *Proc Natl Acad Sci U S A*. 2009;106(18):7559–64.
- Bozdech Z, Llinás M, Pulliam BL, Wong ED, Zhu J, DeRisi JL. The transcriptome of the Intraerythrocytic Developmental cycle of Plasmodium Falciparum. *PLoS Biol*. 2003;1(1): e5.
- Tonkin-Hill GQ, Trianty L, Noviyanti R, Nguyen HHT, Sebayang BF, Lampah DA, et al. The Plasmodium falciparum transcriptome in severe malaria reveals altered expression of genes involved in important processes including surface antigen-encoding var genes. *PLoS Biol*. 2018;16(3):e2004328.
- López-Barragán MJ, Lemieux J, Quiñones M, Williamson KC, Molina-Cruz A, Cui K, et al. Directional gene expression and antisense transcripts in sexual and asexual stages of Plasmodium Falciparum. *BMC Genomics*. 2011;12(1):1–13.
- Robinson MD, McCarthy DJ, Smyth GK. edgeR: a Bioconductor package for differential expression analysis of digital gene expression data. *Bioinformatics*. 2010;26(1):139–40.

34. Risso D, Ngai J, Speed TP, Dudoit S. Normalization of RNA-seq data using factor analysis of control genes or samples. *Nat Biotechnol.* 2014;32(9):896–902.
35. Ewels PA, Peltzer A, Fillinger S, Patel H, Alneberg J, Wilm A, et al. The nf-core framework for community-curated bioinformatics pipelines. *Nat Biotechnol.* 2020;38(3):276–8.
36. Dobin A, Davis C, Schlesinger F, Drenkow J, Chris Z, Jha S. Bioinformatics. 2013 [cited 2020 May 21]. p. 15–21 STAR: ultrafast universal RNA-seq aligner. Available from: <https://www.ncbi.nlm.nih.gov/pmc/articles/PMC3530905/>
37. Li B, Dewey CN. RSEM: accurate transcript quantification from RNA-Seq data with or without a reference genome. *BMC Bioinformatics.* 2011;12:323.
38. Harrington CA, Fei SS, Minnier J, Carbone L, Searles R, Davis BA, et al. RNA-Seq of human whole blood: Evaluation of globin RNA depletion on Ribo-Zero library method. *Scientific Reports.* 2020;10(1):1–12.
39. Kanehisa M, Goto S. KEGG- Kyoto encyclopedia of genes and genomes. *Nucleic Acids Res.* 2000;28(1):27–30.
40. Yu G, Wang LG, Han Y, He QY. ClusterProfiler: an R package for comparing biological themes among gene clusters. *OMICS.* 2012;16(5):284–7.
41. Chen B, Khodadoust MS, Liu CL, Newman AM, Alizadeh AA. Profiling tumor infiltrating immune cells with CIBERSORT. *Methods Mol Biol.* 2018;1711:243–59.
42. Newman AM, Liu CL, Green MR, Gentles AJ, Feng W, Xu Y, et al. Robust enumeration of cell subsets from tissue expression profiles. *Nature Methods.* 2015;12(5):453–7.
43. Njunge JM, Gwela A, Kibinge NK, Ngari M, Nyamako L, Nyatichi E, et al. Biomarkers of post-discharge mortality among children with complicated severe acute malnutrition. *Sci Rep* 2019. 2019;9(1):1.
44. Cox J, Mann M. MaxQuant enables high peptide identification rates, individualized p.p.b.-range mass accuracies and proteome-wide protein quantification. *Nat Biotechnol.* 2008;26(12):1367–72.
45. Cox J, Neuhauser N, Michalski A, Scheltema RA, Olsen JV, Mann M. Andromeda: a peptide search engine integrated into the MaxQuant environment. *J Proteome Res.* 2011;10(4):1794–805.
46. Tyanova S, Cox J. Perseus: A bioinformatics platform for integrative analysis of proteomics data in cancer research. *Methods in Molecular Biology.* 2018;1711:133–48.
47. Portugal S, Tran TM, Ongoiba A, Bathily A, Li S, Doumbo S, et al. Treatment of chronic asymptomatic plasmodium falciparum infection does not increase the risk of clinical malaria upon reinfection. *Clin Infect Dis.* 2017;64(5):645–53.
48. Guillochon E, Fraering J, Joste V, Kamaliddin C, Vianou B, Houzé L, et al. Transcriptome Analysis of Plasmodium falciparum Isolates From Benin Reveals Specific Gene Expression Associated With Cerebral Malaria. *J Infect Dis.* 2022;225(12):2187–96 (Available from: <https://academic.oup.com/jid/article/225/12/2187/6543891>. Cited 2022 Jul 27).
49. Thomson-Luque R, Votborg-Novél L, Ndovie W, Andrade CM, Niangaly M, Attipa C, et al. Plasmodium Falciparum transcription in different clinical presentations of malaria associates with circulation time of infected erythrocytes. *Nat Commun.* 2021;12(1):4711.
50. Jensen ATR, Magistrado P, Sharp S, Joergensen L, Lavstsen T, Chiu-chiuini A, et al. Plasmodium falciparum associated with severe childhood malaria preferentially expresses PfEMP1 encoded by group a var genes. *J Exp Med.* 2004;199(9):1179–90.
51. Robinson BA, Welch TL, Smith JD. Widespread functional specialization of Plasmodium Falciparum erythrocyte membrane protein 1 family members to bind CD36 analysed across a parasite genome. *Mol Microbiol.* 2003;47(5):1265–78.
52. Singhaboot Y, Keayarsa S, Piaraksa N, Phumratanaprapin W, Kunawut P, Dondorp A, et al. Temperature dependence of Plasmodium Falciparum Erythrocytic Stage Development. *Am J Trop Med Hyg.* 2019;100(5):1191–5.
53. Hubbard AK, Rothlein R. Intercellular adhesion molecule-1 (ICAM-1) expression and cell signaling cascades. *Free Radic Biol Med.* 2000;28(9):1379–86.
54. Tuikue Ndam N, Moussiliou A, Lavstsen T, Kamaliddin C, Jensen ATR, Mama A, et al. Parasites causing cerebral Falciparum Malaria Bind multiple endothelial receptors and express EPCR and ICAM-1-Binding PfEMP1. *J Infect Dis.* 2017;215(12):1918–25.
55. Almelli T, Nuel G, Bischoff E, Aubouy A, Elati M, Wang CW, et al. Differences in Gene Transcriptomic Pattern of Plasmodium falciparum in Children with Cerebral Malaria and Asymptomatic Carriers. *PLoS One.* 2014;9(12):e114401 (Tetteh KKA, editor).
56. Popa GL, Popa MI. Recent advances in understanding the inflammatory response in Malaria: a review of the dual role of cytokines. *J Immunol Res.* 2021;2021:7785180.
57. Ockenhouse CF, Hu WC, Kester KE, Cummings JF, Stewart A, Heppner DG, et al. Common and divergent immune response signaling pathways discovered in peripheral blood mononuclear cell gene expression patterns in presymptomatic and clinically apparent malaria. *Infect Immun.* 2006;74(10):5561–73.
58. Obeng-Adjei N, Portugal S, Tran TM, Yazew TB, Skinner J, Li S, et al. Circulating Th1-Cell-type tfh cells that exhibit impaired B cell help are preferentially activated during Acute Malaria in Children. *Cell Rep.* 2015;13(2):425–39.
59. Ryg-Cornejo V, Ioannidis LJ, Ly A, Chiu CY, Tellier J, Hill DL, et al. Severe Malaria infections Impair Germinal Center responses by inhibiting T follicular helper cell differentiation. *Cell Rep.* 2016;14(1):68–81.
60. Soon MSF, Nalubega M, Boyle MJ. T-follicular helper cells in malaria infection and roles in antibody induction. *Oxf Open Immunol.* 2021;2(1):iqab008.
61. Al-Yaman F, Genton B, Anders RF, Falk M, Triglia T, Lewis D, et al. Relationship between Humoral Response to Plasmodium Falciparum Merozoite Surface Antigen-2 and Malaria Morbidity in a highly endemic area of Papua New Guinea. *Am J Trop Med Hyg.* 1994;51(5):593–602.

## Publisher's Note

Springer Nature remains neutral with regard to jurisdictional claims in published maps and institutional affiliations.